TRANSMIT AND RECEIVE ANTENNA ARRAY GEOMETRIES FOR MODE SELECTIVE HF OTH MIMO RADAR

Yuri I. Abramovich[*], *Gordon J. Frazer*[*] *and Ben A. Johnson*[†]

[†]ISR Division, DSTO, PO Box 1500, Edinburgh SA 5111, Australia
email: (yuri.abramovich, gordon.frazer)@dsto.defence.gov.au
[*] Lockheed Martin Australia, 45 Third Avenue, Mawson Lakes SA 5085, Australia
email: ben.a.johnson@ieee.org

ABSTRACT

Use of multiple transmit waveforms to enable MIMO radar operation is a technology with strong application to HF over-the-horizon (OTH) radar. We consider the problem of target detection when the OTH radar is operating in an environment with a stable ionospheric propagation path supporting high quality Doppler spectra from backscattered signals and clutter, and a perturbed ionospheric propagation path which contaminates the signal with spread-Doppler clutter. In this case, efficient spread-clutter mitigation requires elevation and azimuth beampattern control via 2-D arrays. In addition, due to the propagation geometry, the beampattern control needs to range-dependent for both transmit and receive antenna arrays, mandating the use of the MIMO radar architecture. We examine the impact of antenna geometries on clutter mitigation performance. We also provide performance analysis for a specific configuration employing 1-D transmit and receive antennas which enables field experiments that validate MIMO OTH radar operations.

1. INTRODUCTION

We consider high-frequency (HF) over-the-horizon (OTH, skywave) multiple-input multiple-output (MIMO) radar, where both the (separate) transmit and receive subsystems are arrayed, and the transmitter is able to simultaneously transmit different waveforms from each antenna [1, 2]. In the OTH context, *spread clutter* arises when the radar signal propagates from a transmitter (Tx) to a surface region and/or from the surface region back to a receiver (Rx) via a highly perturbed ionospheric layer, such as the F_2 layer. When the radar range (group delay) of such a radar return coincides with the group delay of the ("proper") target return that is propagated via a different stable ionospheric layer (such as the E or E_s layer), the target is masked by these "spread-clutter" returns. Perturbations in the "unwanted" F_2 layer are common, and cause the Doppler spectrum of these returns to be much broader than the Doppler spectrum of the "cold-clutter" returns propagated together with a target via the stable E or E_s layer.

This means that for any given range-resolution cell (RC) on the surface, we may observe a mixture of the "proper" radar returns supported by stable two-way propagation (i.e. Tx $\rightarrow$ RC $\rightarrow$ Rx via the E or E_s layer, known as "E–E mode") and the unwanted spread-clutter returns supported by E–F, F–E and F–F modes.

In general, this mixture of four different propagation modes comprises returns from *different* patches of the Earth's surface (terrain or ocean), so each patch has a different elevation direction-of-departure (DoD) from the Tx and a different elevation direction-of-arrival (DoA) to the Rx. This is because there is a substantial difference in the typical ionospheric heights of the E or E_s layer (about 100km) and the F_2 layer (about 350km). However, this difference in elevation DoD for the same outgoing modes (E–E and E–F), or in DoA for the same incoming modes (E–F and F–F) is negligible due to the geometry of the overall path, and no practical antenna array would have sufficient (projected) vertical dimension to directly use its resolution capability to resolve these elevation angles. Only the difference in elevation angle between the different modes that leave the Tx (E–F and F–E), or between the different modes that arrive at the Rx (E–E and E–F), can be considered sufficient to be resolved given reasonable dimensions of the 2–D Tx and Rx arrays. The existence of the "mixed" propagation modes E–F and F–E requires *both* Tx and Rx adaptive array processing to successfully mitigate all the three components of the spread clutter (E–F, F–E and F–F).

Another complication is that the elevation angles are range-dependent. For a modern digital receive antenna array, this is not a problem, since each radar range cell can be processed by an individually tailored beamformer. Yet for a conventional single-waveform radar, range-dependent Tx beamforming is not feasible. This fundamental limitation motivates us to investigate the MIMO radar architecture, with its capability of forming "Tx beams" after the waveforms have been transmitted, backscattered and received, i.e. non-causal ("after-the-event") processing [3].

More specifically,a MIMO radar with K Tx elements simultaneously transmits a different and "orthogonal" (separable) waveform from each element. The "orthogonality" of the set of K waveforms allows us to separate each of the K radar returns upon receive. The individual returns can then be linearly combined in a range-dependent fashion, similarly to conventional radar processing.

In our previous studies [4, 5], we were concerned with the fundamental limitations on the maximum range depth and Doppler frequency span that different scatterers (targets, clutter) can occupy in order for the orthogonality requirement to be retained. We found that if we observe a peak at the output of a filter matched to the j^{th} waveform, due to the presence of a point scatterer, there must be no other signals created by different scatterers or waveforms. The physical meaning of these conditions is as follows: the peak of a signal backscattered by some point scatterer (at the output of a filter matched to the j^{th} waveform) has no contribution from other scatterers or other waveforms of the orthogonal set. It is only under this condition that we can directly associate the output of the j^{th} matched filter with the signal transmitted from the j^{th} Tx element. This limitation is fundamental, and is analogous to the famous "vol-

 ISSN 2076-1465

ume clearance" condition for the radar ambiguity function established by Price and Hofstetter [6]. Supposing that this condition is satisfied by the choice of a suitable waveform set, there is still the problem of appropriate Tx and Rx array design in order to successfully mitigate clutter. In this paper, we provide an analysis of the MIMO spread-clutter covariance matrix for various Tx and Rx antenna array geometries, and demonstrate the existence of practical 2-D designs. We then explore the performance of a specific configuration of 1-D arrsy, where the Tx array and Rx array are "crossed", allowing for experimental validation of MIMO radar operation using existing antenna arrays.

2. SPREAD-CLUTTER POWER AT THE OUTPUT OF A MIMO RECEIVER

Let $u_j(t)$ ($j=1,\dots,K$, $t\in\{0,T\}$) be a set of "orthogonal" (separable) waveforms transmitted by K Tx subsystems (sub-arrays, elements, beams, *etc.*), with identical patterns $G_t(\varphi,\theta|\varphi_T,\theta_T)$, steered in azimuth θ_T and elevation φ_T. Let $\{\mathbf{x}_{T_K},\mathbf{y}_{T_K}\}$ ($k=1,\dots,K$) be the coordinates of the phase centres of the K transmitting subsystems. Similarly, let $\{\mathbf{x}_{R_l},\mathbf{y}_{R_l}\}$ ($l=1,\dots,L$) be the coordinates of the L Rx subsystems with identical patterns $G_R(\varphi,\theta|\varphi_0,\theta_0)$, steered in the target direction-of-arrival (DoA) $\{\varphi_0,\theta_0\}$.

We consider conventional dimensions of Tx and Rx antenna arrays, so that the manifold (steering) vectors are

$$E_K(\varphi,\theta)\equiv\exp\left[i\frac{2\pi}{\lambda}(u\mathbf{x}_{T_K}+v\mathbf{y}_{T_K})\right]$$
$$k=1,\dots,K,\quad u\equiv\sin\varphi\cos\theta,\quad v\equiv\sin\varphi\sin\theta \qquad (1)$$

for the transmitting array, and similarly for the receiving array

$$E_L(\varphi,\theta)\equiv\exp\left[i\frac{2\pi}{\lambda}(u'\mathbf{x}_{R_l}+v'\mathbf{y}_{R_l})\right]$$
$$l=1,\dots,L,\quad u'\equiv\sin\varphi'\cos\theta,\quad v'\equiv\sin\varphi'\sin\theta. \qquad (2)$$

Expressions (1) and (2) reflect our assumption on the same azimuth for any point scatterer both for Tx and Rx arrays, with different elevation angle possible.

Consider the $K\times K$ ambiguity matrix of the K-variate waveform set

$$\mathscr{X}(\Delta\tau,\Delta f)=\left\{x_{jk}(\Delta\tau,\Delta f)\right\}_{j,k=1,\dots,K}\text{ where} \qquad (3)$$

$$x_{jk}(\Delta\tau,\Delta f)\equiv\int_{\tau_0}^{T+\tau_0}\bar{u}_j(t-\tau_0)u_k(t-\tau)\exp\left[i2\pi(f-f_0)t\right]dt,$$
$$\Delta\tau=\tau-\tau_0,\quad \Delta f=f-f_0. \qquad (4)$$

Let $W_{KL}=\{w_{kl}\}$ ($l=1,\dots,L$, $k=1,\dots,K$) be the KL-variate vector of MIMO processing, then the power at the output of MIMO receiver for a target with the coordinates $\{\varphi_0,\theta_0,\Delta\tau=0,\Delta f=0\}$ and white noise is

$$(\sigma_t^2)_{out}=\sigma_t^2|G_T(\varphi_0,\theta_0|\varphi_T,\theta_T)|^2|G_R(\varphi_0,\theta_0|\varphi_0,\theta_0)|^2$$
$$\times W_{KL}^H\Big[E_L(\varphi_0,\theta_0)E_L^H(\varphi_0,\theta_0)\otimes\mathscr{X}(0,0)$$
$$E_K(\varphi_0,\theta_0)E_K^H(\varphi_0,\theta_0)\otimes\mathscr{X}^H(0,0)\Big]W_{KL} \qquad (5)$$

$$(\sigma_n^2)_{out}=\sigma_n^2W_{KL}^H\left[I_L\otimes\mathscr{X}(0,0)\right]W_{KL} \qquad (6)$$

where σ_t^2, σ_n^2 are the target, clutter and noise power with considered propagation loss, and $\otimes$ is the symbol for the Kronecker product.

Then the total power of "spread clutter", collected from the target range and Doppler resolution cell (for the F–E mode with uniform clutter distribution across the sector $[-\pi,\pi]$) in the absence of the ambiguity function sidelobes in the area occupied by spread clutter (see [5] for details) is

$$\sigma_c^{F-E}=$$
$$\sigma_c^2\Gamma_0W_{KL}^H\left\{\int_{-\pi}^{\pi}|G_R(\varphi_0,\theta|\varphi_0,\theta_0)|^2|G_T(\varphi_F,\theta|\varphi_T,\theta_T)|^2\times\right.$$
$$\times\Big[E_L(\varphi_0,\theta)E_L^H(\varphi_0,\theta)\otimes\mathscr{X}(0,0)$$
$$\left.E_K(\varphi_F,\theta)E_K^H(\varphi_F,\theta)\mathscr{X}^H(0,0)\Big]d\theta\right\}W_{KL}. \qquad (7)$$

Similar expressions for the E–F mode have DoD $\{\varphi_0,\theta\}$ and DoA $\{\varphi_F,\theta\}$, while for the F–F mode, both DoD and DoA are the same $\{\varphi_F,\theta\}$. Equation (7) prompts us to seek the ideal antenna geometry that retains the rank-one property of the covariance matrix in (7) despite the integration, with all degrees of freedom allocated for resolution in elevation. Indeed, for a target at the azimuth $\theta_0=0$, an antenna array with

$$|G_R(\varphi_0,\theta|\varphi_0,\theta_0)|^2|G_T(\varphi_F,\theta|\varphi_T,\theta_T)|^2$$
$$\to\delta(\sin\varphi_0\sin\theta-\sin\varphi_0\sin\theta_0) \qquad (8)$$

(i.e. that product of norms approaches a delta-function in azimuth), and where

$$\begin{array}{l}E_K(\varphi,\theta)=\left\{\exp\left[i\frac{2\pi}{\lambda}U\mathbf{x}_{T_k}\right]\right\},\quad k=1,\dots,K\\ E_L(\varphi,\theta)=\left\{\exp\left[i\frac{2\pi}{\lambda}U'\mathbf{x}_{R_l}\right]\right\},\quad l=1,\dots,L\end{array} \qquad (9)$$

then the covariance matrix corresponding to the F–E mode in (7) is the rank-one matrix

$$R_{KL}^{F-E}=\hat{\sigma_c}^2|G_T(\varphi_F,\theta_0|\varphi_T,\theta_T)|^2|G_R(\varphi_0,\theta_0|\varphi_0,\theta_0)|^2\times$$
$$\left[E_L(\varphi_0,\theta_0)E_L^H(\varphi_0,\theta_0)\otimes E_K(\varphi_F,\theta_0)E_K(\varphi_F,\theta_0)\right]. \qquad (10)$$

This means that for a given look direction, say $\theta_0=0$, the optimum antenna array geometry could be interpreted as Tx and Rx rectangular arrays with $\theta_0=0$ in the boresight, with the number of elements N_T or N_R in each of the K (for Tx) or L (for Rx) linear arrays tending to infinity $\max\{N_T,N_R\}\to\infty$, so that (8) is satisfied. Practically though, the rectangular arrays with K and L rows correspondingly, may have only a limited number of sensors in a row (limited ULA aperture), and have to cover a certain azimuthal sector. Moreover, these 2-D antennas may have insufficient front-to-back ratio of its elements, or intentionally be designed to cover front and back sectors simultaneously.

Therefore, analysis of the actual spread clutter potential mitigation capability is required, with respect to the practical (limited) antenna aperture and azimuthal coverage.

3. ANALYSIS OF SPREAD-CLUTTER MITIGATION FOR PRACTICAL 2–D ANTENNA GEOMETRIES

Potential spread-clutter mitigation efficiency analysis has been performed using expression (7) for the Tx and Rx beampatterns ap-

proximated as

$$G_T(\varphi_F,\theta|\varphi_T,\theta_T)|^2 = \\ = G_T^2 \exp\left\{-b_T\left[(\sin\varphi_F\sin\theta-\sin\varphi_T\sin\theta_T)\right]^2\right\} \quad (11)$$

$$G_R(\varphi_0,\theta|\varphi_0,\theta_0)|^2 = \\ = G_R^2 \exp\left\{-b_R\left[\sin\varphi_0(\sin\theta-\sin\theta_T)\right]^2\right\}. \quad (12)$$

Calculations have been performed for a typical E-mode HF OTHR scenario

$$\begin{array}{ll}\varphi_0^{E-E}(Z_{min})=79^o, & \varphi_0^{E-E}(Z_{max})=87^o,\\ \varphi_F^{E-E}(Z_{min})=51^o, & \varphi_F^{E-E}(Z_{max})=75^o.\end{array} \quad (13)$$

We consider the case where the elements have an ideal front-to-back ratio which attenuates returns from the back hemisphere of the array.

In order to obtain the required resolution in the maximum range regime, the "in-depth" dimension of the Tx array is chosen to be 70λ, being spanned by either (a) an 8-element ULA with element spacing d_{2T}/λ=10, or (b) an 8-element non-redundant array (NRA) with unit spacing d_{2T}/λ=2 and geometry $[0,7,10,16,18,30,31,35]$.

For the Rx antenna array, we consider $L=16$ "rows" with either (a) ULA with spacing $d_{2R}/\lambda=5$, or (b) NRA geometry with the unit spacing $d_{2R}/\lambda=3/7$. Note that the traditional spacing $d_{2R}/\lambda=1/2$ causes ambiguity in front-to-back resolution for extreme end-fire directions, such as $\varphi_0=87^o$. We selected the geometry of the Rx "vertical" $L=16$-element array to be [0, 6, 19, 40, 58, 67, 78, 83, 109, 132, 133, 162, 165, 169, 177, 179].

It is simple to show that at the maximum range ($\phi_0=87^\circ$, $\phi_F=75^\circ$), the large uniform spacing in the Tx array does not create a problem, but is inappropriate at the minimum range. Indeed, the "to-be-rejected" direction $\phi_F=75^\circ$ is already outside the main peak of the beampattern steered at the elevation angle $\phi_0=87^\circ$, but has not yet reached the direction of the nearest grating lobe at $\phi_{gl}=71.5^\circ$. On the contrary, at the minimum range ($\phi_0=79^\circ$, $\phi_F=51^\circ$), even the $d_{2R}/\lambda=5$ uniform inter-row separation in the 16-row Rx array is too large, since when the main peak is steered at the target elevation $\phi_0=79^\circ$, the nearest grating lobe is observed at $\phi_{gl}=69^\circ$, which is much closer than $\phi_F=51^\circ$. The introduced NRA geometries address this problem, as the first grating lobe of our 8-element NRA with the unit spacing $d_{2T}/\lambda=2$ is observed at $\phi_{gl}=43^\circ$, when the array is steered at the target elevation at the minimum distance $\phi_0(r_{\min})=79^\circ$, since here $\phi_{gl}<\phi_F$.

Note that due to the chosen unit separation $d_{2R}/\lambda<0.5$, our Rx array does not have grating lobes in the visible domain, even when steered to the extreme end fire direction $\phi_0=90^\circ$. However both 8- and 16-element NRA arrays have a significant sidelobe level, which will affect the performance of adaptive spread-clutter mitigation.

In order to evaluate the additional penalty in spread-clutter mitigation efficiency that is introduced by a high sidelobe level of the selected NRAs, we compare the ULA and NRA geometries at the maximum range, where the uniform array geometry is still appropriate. A similar comparison at the minimum range, on the contrary, demonstrates the improvements introduced by an NRA geometry.

3.1 Ideal Front-to-Back Ratio in Either or Both the Tx and Rx Elements

In our calculations, the equivalent noise power is set to one ($\sigma_n^2\chi_{uu}(0,0)=1$) and the spread-clutter-to-noise ratio per mode is 30 dB. Hence if the clutter is rejected with no signal-to-white-noise ratio (SNR) losses, the maximum possible SNR at the output of our MIMO receiver is $\mathrm{SNR}_{\max}=10\log KL=10\log 128=21.07$dB. The upper plot in Fig. 1 shows, for the uniform ("vertical") Tx and Rx array geometry and at the maximum range ($\phi_0=87^\circ$, $\phi_F=75^\circ$), the output SNR for the optimum (clairvoyant) Wiener filter calculated for each of the three spread-clutter mode contributions (E–F, F–E and F–F), and for the sum of all three covariance matrices. In other words, in addition to all three modes together, we also illustrate the efficiency of each single-mode mitigation, as if only this mode was present. Similarly, the lower plot presents the gain of the optimum clairvoyant Wiener MIMO receiver with respect to the conventional (white-noise) matched receiver (i.e. gain wrt CBF): In order to evaluate the impact of "eigenspectrum smearing" (spreading), for all three interference modes contributing, Fig. 1 also plots the SNR and SNR gain with respect to the matched filter for the rank-one contributions in (10) (curve labeled "3 modes no sm").

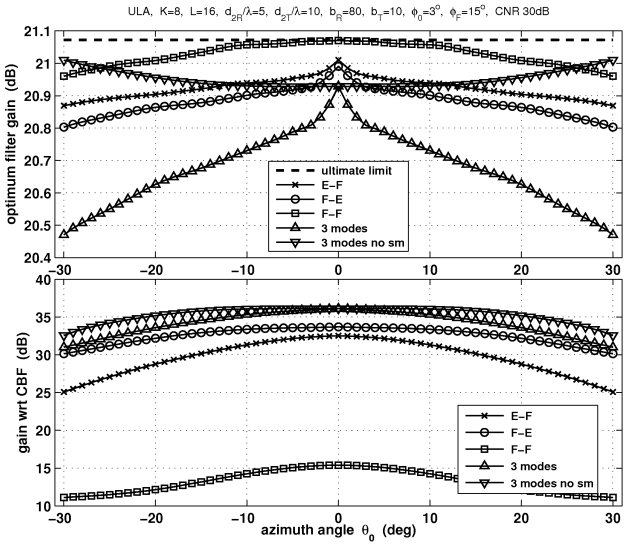

Figure 1: Simulation results for the 2-D ULA at maximum range.

As expected, in the bore sight direction $\theta_0=0$, no difference between this rank-one and the "full-rank" model (7) exists, but as θ_0 grows, the difference between the rank-one and full-rank covariance matrices becomes evident. In fact, the SNR for the rank-one model even increases slightly as $\theta_0\to 30^\circ$, while the full-rank SNR obviously degrades. However, within the entire sector of our interest ($|\theta_0|<30^\circ$), the SNR losses with respect to the ultimate limit of 21.1 dB remain extremely low: less than 1.2 dB. Both the Tx and Rx participate in mitigating F–F spread clutter, whereas only the Tx is involved in reducing F–E mode clutter and only the Rx is involved in reducing E–F mode clutter, so it is expected to see that the F–F mode is better rejected than the E–F and F–E modes; with E–F being rejected better than F–E, since only 8 degrees of freedom of our Tx MIMO array are used. Not surprisingly, the gain with respect to the matched receiver (in Fig. 1(b)) remains above 30 dB within the entire coverage.

Unfortunately for the horizontal 2D array, a uniform geometry is inappropriate, as seen in [7]. There it was shown that as the grating lobes enter the azimuthal coverage, the optimum receiver has no gain over the matched filter; this is typical behavior for interference that impinges upon the maximum of a grating lobe. So as predicted, a ULA geometry with extremely large inter-row separation (10λ in Tx and 5λ in Rx), cannot be used if the entire range interval from $r_{\min}$ to $r_{\max}$ is to be covered.

We now analyze the results of our example NRA geometry. We start from the maximum range ($\phi_0 = 87^\circ$, $\phi_F = 75^\circ$), where we can quantify the losses associated with the very high sidelobe level in our 8-element Tx NRA (-3.5 dB) and 16-element Rx NRA (-4.6 dB). From Fig. 3, it is clear that rejection of the much higher sidelobes of the NRA patterns causes additional SNR degradation that is less than 1.6 dB. Therefore, with respect to the ultimate limit of 21.1 dB that corresponds to the case with no spread clutter, we observe SNRs ranging from 20.1 dB at $\theta_0 = 0$ to 18.9 dB at $\theta_0 = \pm 30^\circ$.

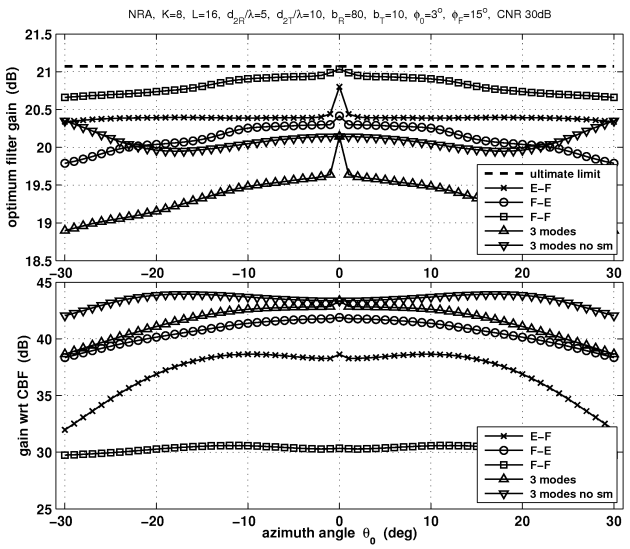

Figure 2: Simulation results for the 2-D NLA at maximum range.

At the same time, the SNR gain with respect to the matched filter remains much higher than at Fig. 1 for the uniform geometry (above 40 dB). Given a quite poor NRA beampattern sidelobe level, such a poor performance of the matched receiver and, correspondingly, high gains of the optimal MIMO receiver, are not surprising.

Therefore, the suggested Tx and Rx NRA-based array geometries with ideal front-to-back ratio have a very high potential efficiency of spread-clutter mitigation within the entire range depth and azimuth coverage. In [7] we demonstrated that for ommidirectional array elements, we have to ultimately consider seven modes impinging upon a receive antenna from both front and back hemispheres, instead of only three ones from the front hemisphere only. Analysis in [7] showed that the SNR degradation is less than 2dB, while the SNR gains with respect to the matched filter remain high ($\sim$40dB).

3.2 Experimental mode-selective OTH MIMO radar configuration with one-dimensional Tx and Rx antennas

Experimental validation of mode-selective HF OTH MIMO radar principles may obviously be considered within a relatively limited coverage in range and azimuth. For end-fire linear Tx and linear Rx antennas with relatively large apertures, such a limited coverage may be introduced by exploiting the difference in coning angles of differently oriented Tx and Rx linear arrays.

Let us consider a case when the end-fire direction of the Tx array coincides with the broadside (boresight) direction of the Rx linear array. Then, for relatively close in ranges with

$$\varphi_F^{E-F} \ll \varphi_0^{E-E}, \tag{14}$$

we can specify such an azimuth direction θ_0 that due to the coning equation

$$\sin\varphi_F^{E-F} \sin\theta_F^{E-F} = \sin\varphi_0^{E-E} \sin\theta_0^{E-E} \tag{15}$$

the actual clutter patch on the ocean surface, contributing to spread clutter delivered to the receiver array via the E-F propagation mode, would be actually coming from the azimuth $\theta_F^{E-F} \gg \theta_0^{E-E}$. Therefore, if the aperture of the end-fire Tx array is large enough to enable adaptive MIMO beampattern sidelobe rejection in directions $(\varphi_F, \theta_0^{E-F})$ (for F-E mode), $(\varphi_F, \theta_0^{F-F})$ (for F-F mode), and $(\varphi_E, \theta_F^{E-F})$ (for E-F mode), while retaining low gain degradation in the target direction $(\varphi_E, \theta_F^{E-E})$, then all three spread clutter components may get rejected by means of adaptive Tx MIMO beamforming only.

Naturally, a large Rx linear array aperture is required to retain low "smearing" of the clutter covariance matrix. The obvious appeal of such a configuration is that mode-selective adaptive MIMO principles may be tested using existing HF OTHR receive antennas rather than construction of new 2-D receiver array configurations.

For the considered above scenario at minimal range and with a Tx endfire array with an aperture of 70λ, optimum filter gains as a function of θ_0, is illustrated by Fig. 3. As expected, no spread clutter mitigation is observed at the sector close to the Rx antenna boresight, but off the boresight, there is a considerable sector where sufficiently high performance may be observed.

Indeed, comparison of the optimum signal to clutter-plus-noise ratio (SCNR), delivered by the optimum MIMO Tx beamformer at Fig. 3, with the $(\text{SCNR})^{-1}$ for the conventional beamformer (Fig. 4), and finally, with the improvement in SCNR delivered by the optimal MIMO processing with respect to the conventional beamformer (Fig. 5), supports such a conclusion. Indeed, though the SCNR never approaches its ultimate value of $10\log_{10}(8) = 9$dB, in a sector close to $\theta = 20^o$, we achieve an SCNR of 4dB, which is almost 15 dB above the SCNR in the conventional beamformer at this sector. This margin may be treated as sufficient for experimental validation of mode selection capabilities in HF MIMO radar.

4. SUMMARY AND CONCLUSIONS

In this paper we considered the problem of both transmit and receive antenna geometry selection for spread-clutter mitigation in HF OTH MIMO radar. We demonstrated that the rank of spread-clutter contribution via a particular propagation mode (E–F, F–E or F–F) tends to one, if both Tx and Rx arrays consists of K and L "rows" of linear arrays with forward-only looking elements, and an aperture in either the Tx or Rx linear array that tends to infinity. When K orthogonal waveforms are deployed over the conventionally beam steered K linear arrays of the Tx, and the azimuthal beam width of the Rx linear array tends to zero as its aperture tends to infinity, the

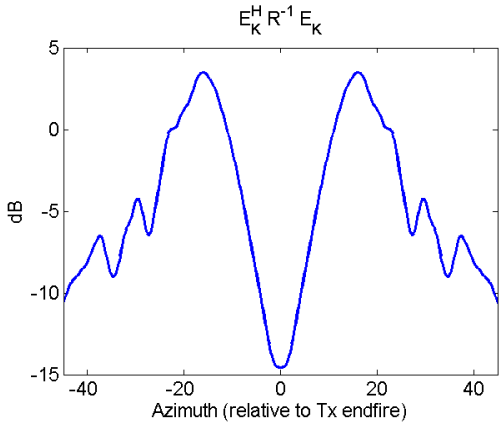

Figure 3: Optimal 1-D Tx/Rx filter results at minimum range.

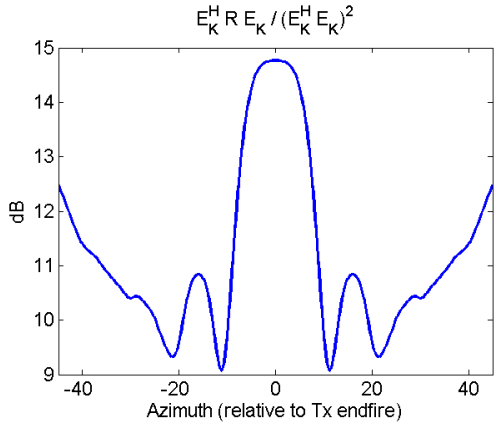

Figure 4: Conventional 1-D Tx/Rx filter results at minimum range.

"elevation rank" of each spread-clutter mode is kept equal to one, despite a broad azimuthal distribution of spread clutter.

Practical array design with a finite aperture of the Rx linear arrays introduces "rank expansion" of the spread-clutter covariance matrix, that depends on the azimuth of the look-direction with respect to the linear array's bore sight.

The SNR performance of the clairvoyant optimal Wiener receiver has been analyzed for different Tx and Rx 2D array geometries, with both forward-only looking and omni-directional elements. It was demonstrated that in order to keep the number K of the waveforms and rows in the Tx array small, and yet to provide the required resolution within the entire "range depth" of the radar coverage, sparse non-redundant arrays geometries must be used for the inter-row distance selection in both Tx and Rx arrays.

Such design precludes the grating lobes from entering the directions of rejection, while performance degradation caused by a higher level of NRA sidelobes is shown to be acceptable. Specifically, the conducted analysis demonstrates that for forward-looking arrays, the selected geometry of the Tx and Rx arrays has only 2–2.5 dB SNR degradation compared with the ultimate white-noise limit. In all these cases, the spread clutter is mitigated ~40 dB with respect to white-noise matched conventional Tx and Rx beamforming in the 2D arrays.

We also considered experimental validation of the mode selective capability of a MIMO radar architecture using one-dimensional Tx and Rx antennas, due to the difference in coning angles of differently oriented Tx and Rx linear arrays. We demonstrated that for significantly different elevation angles for E-E and E-F modes (observed at minimal ranges), one can select a limited azimuth sector where spread clutter mitigation associated with mode selection can be clearly demonstrated.

Figure 5: 1-D Tx/Rx SINR Improvement results at minimum range.

REFERENCES

[1] G. Frazer, Y. Abramovich, and B. Johnson, "HF skywave MIMO radar: the HiLoW experimental program," in *Proc. Asilomar-2008*, Pacific Grove, CA, USA, Nov 2008, pp. 639–643.

[2] V. Mecca, J. Krolik, F. Robey, and D. Ramakrishnan, "*Slow-time MIMO spacetime adaptive processing*," in *MIMO Radar Signal Processing*, J. Li and P. Stoica, Eds. Wiley, 2009, ch. 7, pp. 283–318.

[3] G. Frazer, Y. Abramovich, and B. Johnson, "Use of adaptive non-causal transmit beamforming in OTHR: experimental results," in *Proc. RADAR-2008*, Adelaide, Australia, 2008, pp. 311–316.

[4] Y. Abramovich and G. Frazer, "Bounds on the volume and height distributions for the MIMO radar ambiguity function," *IEEE Sig. Proc. Letters*, vol. 15, no. 1, pp. 505–508, 2008.

[5] ——, "MIMO radar performance in clutter: limitations imposed by bounds on the volume and height distributions for the MIMO radar ambiguity function," in *Proc. SAM-2008*, Darmstadt, Germany, 2008, pp. 441–445.

[6] R. Price and E. Hofstetter, "Bounds on the volume and height distributions of the ambiguity function," *IEEE Trans. Info. Theory*, vol. 11, pp. 207–214, Apr. 1965.

[7] Y. I. Abramovich, G. J. Frazer, and B. A. Johnson, "Transmit and receive antenna array geometry design for spread-clutter mitigation in HF OTH MIMO radar," in *Proc. International Radar Symposium*, Hamburg, Germany, 9-11 Sept 2009, pp. 1–5.